Hindawi Publishing Corporation
International Journal of Antennas and Propagation
Volume 2016, Article ID 9734781, 9 pages
http://dx.doi.org/10.1155/2016/9734781

Research Article

A Compact Dielectric Resonator Antenna Excited by a Planar Monopole Patch for Wideband Applications

Xuping Li,[1] Yabing Yang,[2] Fei Gao,[3,4] Hanqing Ma,[2] and Xiaowei Shi[1]

[1] *Key Laboratory of Antennas and Microwave Technology, Xidian University, Xi'an, Shaanxi 710071, China*
[2] *Xi'an Electronic Engineering Research Institute, Xi'an, Shaanxi 710100, China*
[3] *University of California, San Diego, 9500 Gilman Drive, La Jolla, CA 92093, USA*
[4] *Xidian University, Xi'an, Shaanxi 710071, China*

Correspondence should be addressed to Xuping Li; antenna206@163.com

Received 31 August 2015; Revised 29 November 2015; Accepted 16 February 2016

Academic Editor: N. Nasimuddin

Copyright © 2016 Xuping Li et al. This is an open access article distributed under the Creative Commons Attribution License, which permits unrestricted use, distribution, and reproduction in any medium, provided the original work is properly cited.

A compact dielectric resonator antenna (DRA) suitable for wideband applications is presented in this paper. The proposed antenna is mainly composed by a notched cylindrical dielectric resonator (DR) coated with a metal surface on the top and a finite ground plane where the presented DR is placed. This antenna is very simple in structure and has a very low overall height of $0.14\lambda_{\min}$ at its lowest operation frequency. A comprehensive parametric study is carried out based on Ansoft HFSS to optimize the bandwidth. The proposed antenna has been successfully simulated, optimized, fabricated, and measured. The measurement results demonstrate that the proposed design produces an impedance bandwidth of more than 75%, ranging from 2.9 GHz to 6.7 GHz for the reflection coefficient less than −10 dB. In particular, consistent broadside radiation patterns, stable gain, and high radiation efficiency are also obtained within the operation frequency band.

1. Introduction

Since the use of dielectric resonator (DR) as an antenna was originally introduced in the 1980s [1], dielectric resonator antennas (DRAs) have received increasing attention due to several attractive characteristics, such as high radiation efficiency, considerable bandwidth, light weight, small size, and low profile [2, 3]. The DRAs can be designed with various shapes and excited by diversity of feeding mechanisms [4]. Thus, DRAs that possess a high degree of design flexibility have emerged as an ideal candidate for wideband, high efficiency, and cost-effective applications. They are quite useful for high frequency applications, where ohmic losses tend to be a serious problem for conventional metallic antennas [5]. As we know, many existing and emerging wireless communication applications operate over wide frequency bands and thus require broadband antennas. Moreover, the high power capability and high radiation efficiency of such an antenna are considered as an advantage when to be used.

Many investigations have been reported on the development of the DRAs. In the last three decades, one major aspect of the research has been focused on the bandwidth and various techniques have been adopted to broaden operation bandwidth. It is well known that a DRA exhibits a broader operating bandwidth if its Q-factor is lower. In [6], by lifting a DR above the ground plane, its Q-factor can be effectively reduced and exhibited a broader bandwidth. The bandwidth of a DR can also be increased by modifying its geometry. For example, by using a DR with an optimized H-shaped cross section, an impedance bandwidth of about 62% is achieved [7]. A T-shaped DRA with two equilateral-triangle cross sections can reach a bandwidth of more than 60% [8]. Some special geometry of DRs can also enhance the bandwidth, such as conical, biconical, triangle, or other special shape DRs. However, these methods of impedance bandwidth enhancement are nearly at expense of the complex DR structure. Multiple DRs with adjacent resonant frequencies can exhibit broadband characteristics by coupling their resonant modes. In [9], by introducing a full-length lower-permittivity insert between the DR and the ground plane, the realized band covers the FCC UWB band from 3.1 GHz to 10.6 GHz and this method is equivalent to reducing the

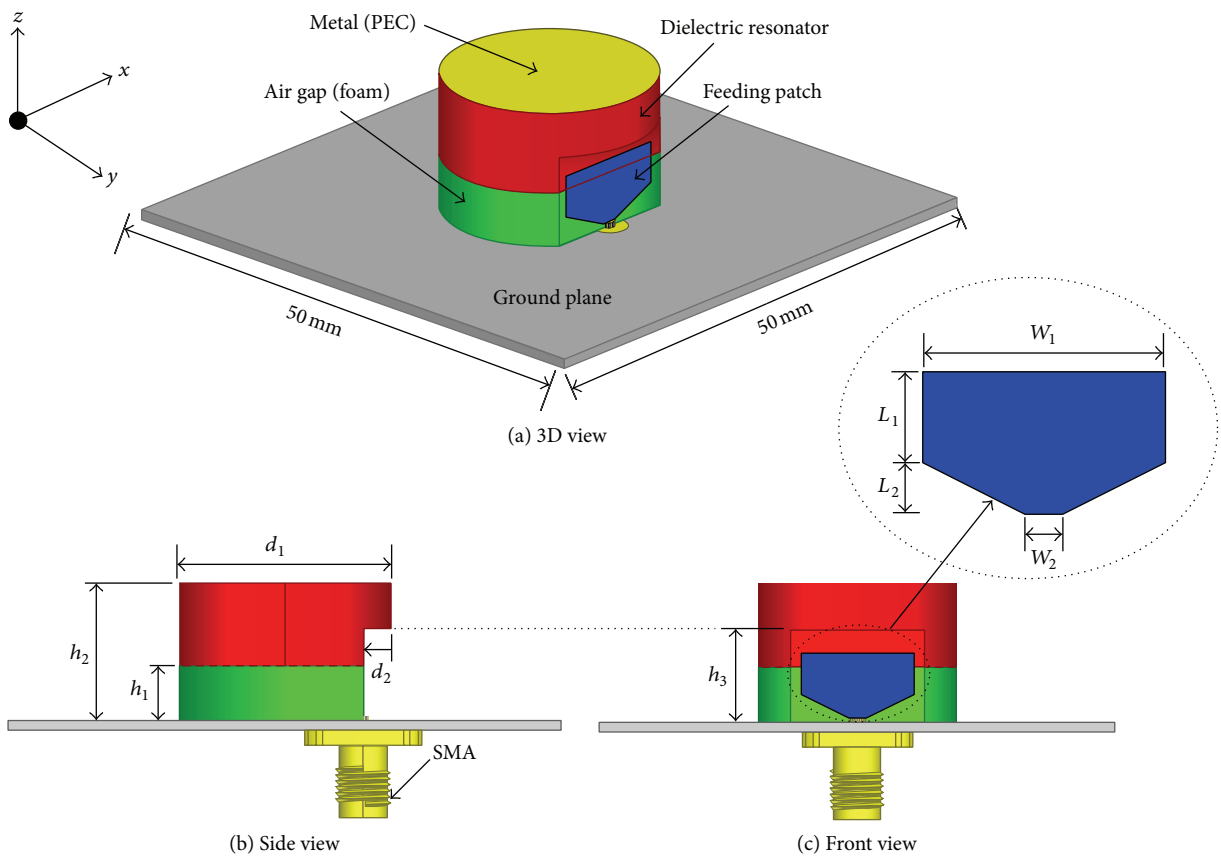

Figure 1: Geometry and configuration of the proposed DRA.

Q-factor. Three methods of a Z-shaped dielectric resonator, a bevel feeding patch, and an air gap are used to obtain an ultrawideband impedance bandwidth of about 120% [10]. But the radiation pattern varies over the band due to the hybrid structure; especially at the higher band the radiation patterns are not consistent and have some deformation. In addition, the impedance bandwidth of DRAs can be further increased by modifying their feeding structures [11–13]. The performance of DRAs is very sensitive to feeding methods. A slight change of the feeding position may cause a big shift of the antenna characteristic. Therefore, the feeding structure plays a crucial role in advanced DRA design.

In this paper, a compact wideband DRA with low profile is presented, which uses a notched cylindrical DR coated with a PEC on the top surface, and a modified trapezoidal monopole patch excitation together with an air gap inserting technique. By applying these methods, desired electromagnetic fields are effectively excited over a broad frequency range. The total bandwidth is a cumulative effect of two types of resonances: one is from the feeding monopole patch and the other from the notched DR. Measured results and simulated ones were carried out and compared, showing a good agreement. With the proposed design, the DRA achieved an impedance bandwidth of more than 75%, and it provides a consistent radiation pattern with a gain range of 4.8 dBi~6.5 dBi across the operating frequency band. Furthermore, the radiation efficiency of the DRA is above 80%, so the DRA works with very high efficiency. Details of the antenna design are described, and experimental results such as the reflection coefficient, the radiation patterns, antenna gain, and radiation efficiency are presented and discussed in the following sections.

2. Antenna Design and Configuration

Figure 1 shows the geometry and configuration of the proposed DRA. The fabricated antenna prototype has electrical dimensions of $0.48\lambda_{\min}\times 0.48\lambda_{\min}\times 0.14\lambda_{\min}$ at its lowest operation frequency. The notched cylindrical DR is centrally placed above a finite ground plane with a size of 50 mm × 50 mm. The proposed DR is depicted by d_1, d_2, h_2, and h_3, which is fabricated on the microwave dielectric material TMM10i with relative permittivity of $\varepsilon_r = 9.8$ and dielectric loss tangent of $\tan\delta < 0.002$. The feeding mechanism adopts a modified trapezoidal patch adhered on the DR concave surface and connected to a 50-Ω SMA connector. The exciting patch has a top width W_1, a bottom width W_2, and lengths of L_1 and L_2. The thickness of the air gap inserted between the DR and the ground plane is denoted by h_1, and the air gap is filled with foam with dielectric constant approximate approaching 1.0.

As shown in Figure 1, the DR which has the thickness of $(h_2 - h_1)$ is coated with a metal on its top surface. Since the permittivity of the dielectric is much higher than that of the air, the dielectric-air interface can be approximated as a

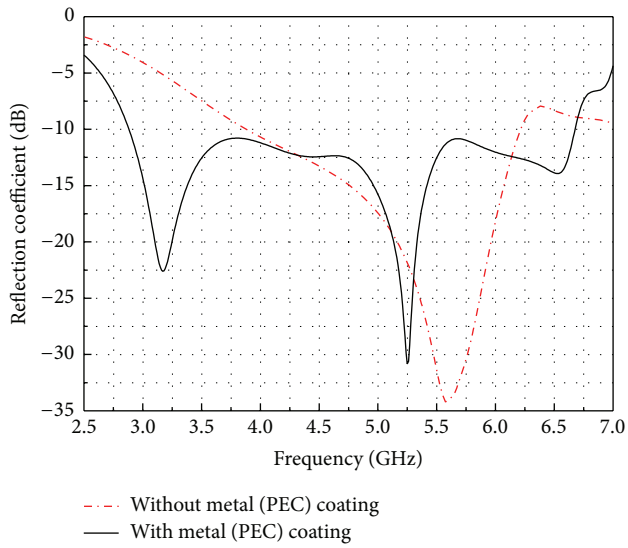

Figure 2: Effect of the metal coating on the impedance matching characteristic.

PMC boundary, and the metal coating is treated as a PEC boundary. Hence, the structure is a cavity with PMC and PEC on different portions of the DR, filled with high-permittivity dielectric. To verify the correctness of the analysis, the simulation results are compared between the proposed antenna with and without the metal coating. As is illustrated in Figure 2, the coated metal on the top leads to another adjacent resonance, and thus the operating bandwidth can be significantly improved.

Figure 3 plots the electric field distributions of the proposed DRA at three different frequencies, where the fundamental mode can be clearly observed due to the notched cylindrical DR and the trapezoidal patch excitation. From the E-field distributions, it is found that the vertical E-field components are much stronger at the lower frequency band. In the E-plane (yz-plane), the vertical and horizontal E-field components, respectively, contribute to the copolarization and cross-polarization radiation, while, in the H-plane (xz-plane), the vertical and horizontal E-field components together contribute to the copolarization radiation. Figure 4 presents the current distribution of the metal (PEC) coating at frequencies 3.0 GHz, 5.0 GHz, and 6.5 GHz. As shown, the surface current distributes uniformly all along the PEC coating but has a little disturbance at higher frequency. It is worth mentioning here that the desired TE_{111} mode is excited effectively.

In theory, the DRAs with a dielectric constant of $\varepsilon_r = 1.0$ have the lowest Q-factor and therefore the widest bandwidth. However, in practice, there is a lower limit on the value of the dielectric constant required to contain the fields within the DRA in order to resonate. As a result, a relative permittivity of $\varepsilon_r = 9.8$, which is close to the practical lower bound for DRAs, is chosen for the design. In this contribution, three different techniques are introduced to enhance the bandwidth of the proposed DRA.

Table 1: Parameters for the optimized DRA (unit: mm).

d_1	d_2	h_1	h_2	h_3	W_1	W_2	L_1	L_2
23.0	3.0	6.0	15.0	10.0	13.0	2.0	4.5	2.5

(a) Firstly, an air gap is formed between the DR and the ground, which contributes to reducing Q-factor and enhancing impedance bandwidth.

(b) Secondly, the feeding patch is trapezoidal, which results in a smooth transition of the impedance from one resonant mode to another and ensures good impedance match in a broad frequency range. The coupling between the DR and the feeding mechanism can be easily adjusted by changing the size of the exciting patch; thus a wideband impedance matching can be obtained.

(c) Finally, a considerable degree of realization over the desired bandwidth is controllable by notching the shape of the DRA, and the notch portion can be denoted by d_2 and h_3.

In our design, the DRA performances were analyzed by using 3D full-wave electromagnetic simulation software Ansoft HFSS, which is based on the finite element method (FEM). Based on the tuning and optimization functions of the software, the proposed antenna was investigated, and the desired wideband DRA design was obtained. The finally optimized dimensions of the proposed DRA are listed in Table 1.

3. Parametric Study

Every geometrical parameter has different effects on the overall performances of the proposed antenna. To better understand the DRA impedance matching characteristic with the variation of some special parameters, in the following section, a parametric study of the designed DRA about the reflection coefficient was performed, which is usually very helpful to our practical antenna designs. The initial values of the design parameters are chosen, as illustrated in Table 1.

3.1. The Thickness of the Air Gap: h_1. The air gap with a thickness h_1 between the DR and the ground plane plays an important role in the bandwidth enhancement. Figure 5 shows the effects of different values of h_1 on the matching over a bandwidth ranging from 2.5 GHz to 7.0 GHz. It can be noticed that, by introducing an air gap, the dual resonances are enhanced and coupled to each other. These results provide evidence that the bandwidth of a DRA can be greatly enhanced by introducing a proper air gap. In addition, we can conclude that when the DR is lifted from the ground plane for more than 5.0 mm, it acts more like an isolated DR.

3.2. The Length of the Feeding Patch: L_1. To investigate the effects of the monopole patch feeding mechanism, Figure 6 shows the simulated reflection coefficient of the DRA for various L_1. It is evident that, by increasing the length of L_1, the impedance matching at the lower frequency band is improved, and the lower edge frequency is slightly reduced.

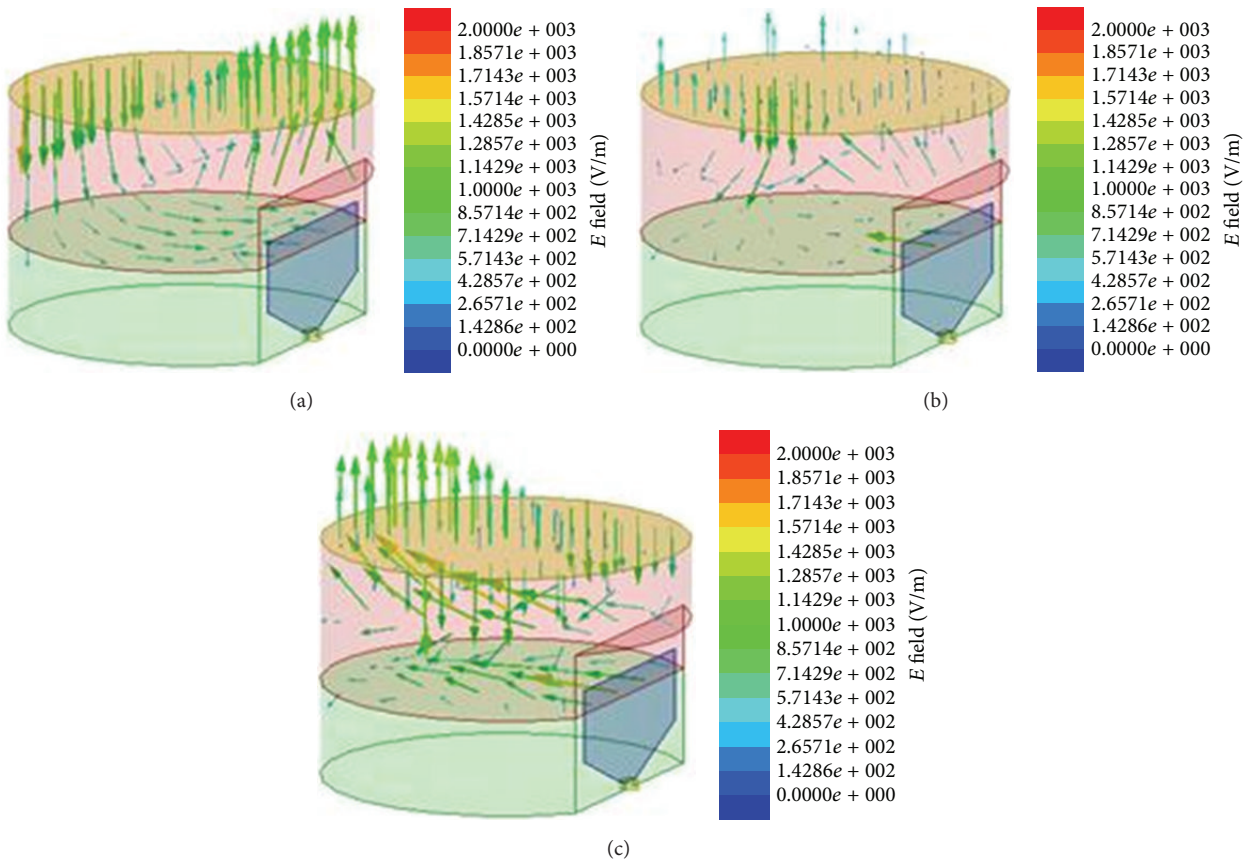

Figure 3: Electrical field distribution of the proposed DRA. (a) 3.0 GHz, (b) 5.0 GHz, and (c) 6.5 GHz.

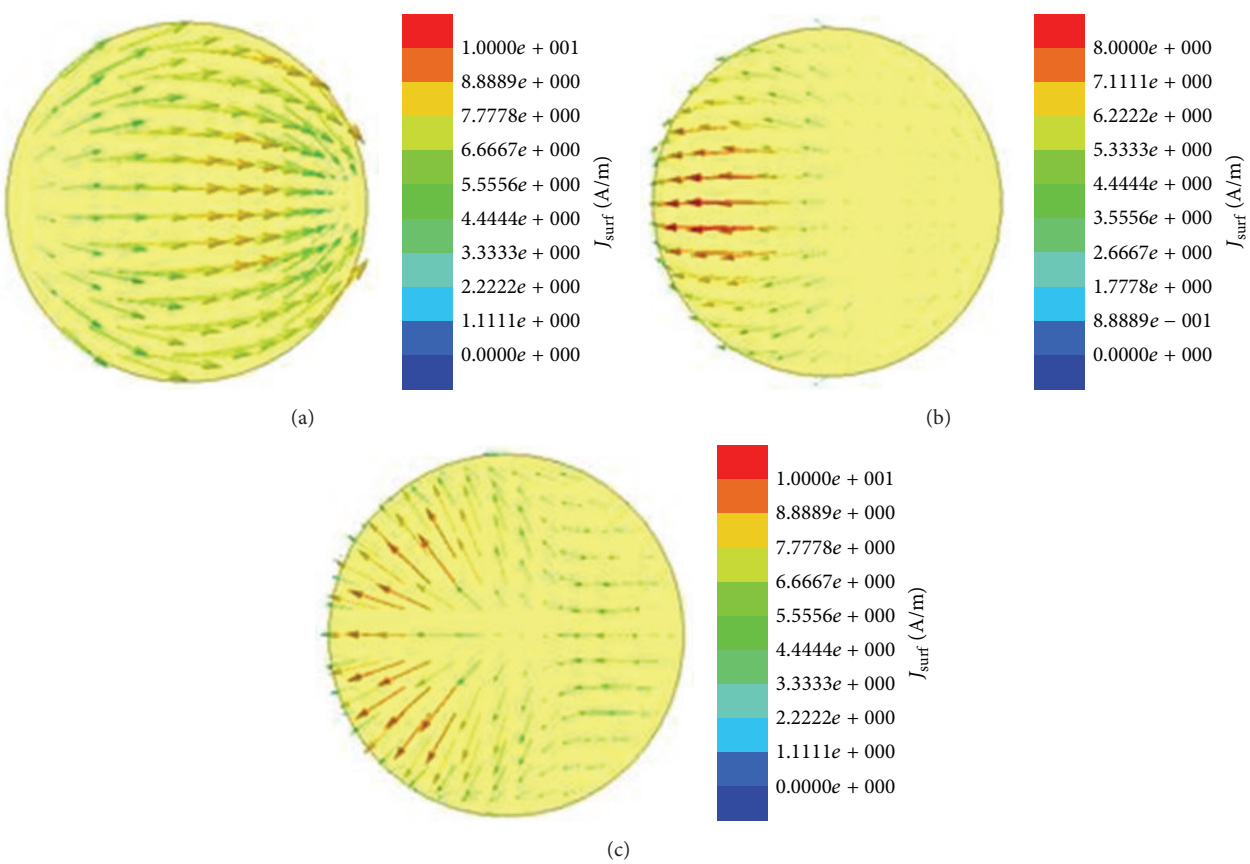

Figure 4: Current distribution of the metal (PEC) coating. (a) 3.0 GHz, (b) 5.0 GHz, and (c) 6.5 GHz.

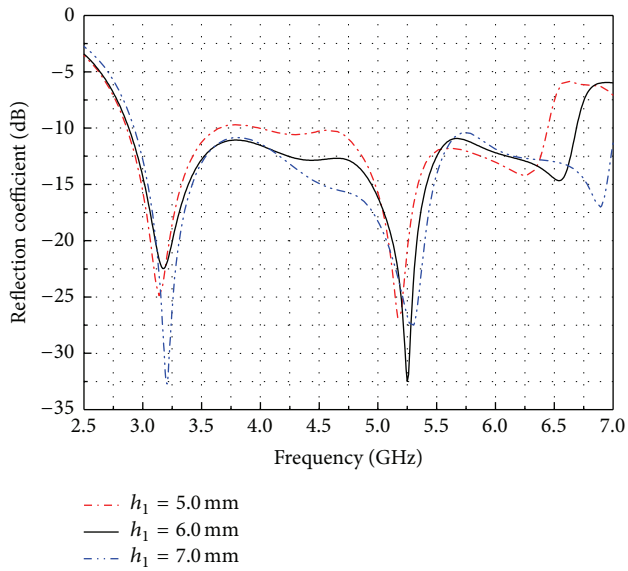

FIGURE 5: Simulated reflection coefficient with different values of h_1 (d_1 = 23.0 mm, d_2 = 3.0 mm, h_2 = 15.0 mm, h_3 = 10.0 mm, W_1 = 13.0 mm, W_2 = 2.0 mm, L_1 = 4.5 mm, and L_2 = 2.5 mm).

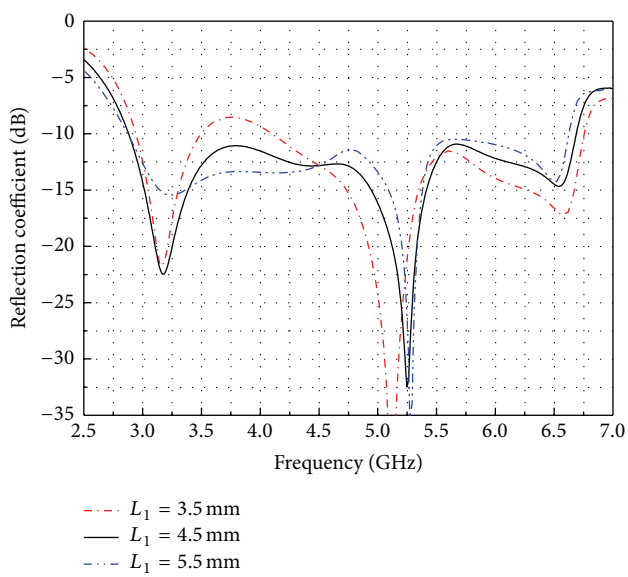

FIGURE 6: Simulated reflection coefficient with different values of L_1 (d_1 = 23.0 mm, d_2 = 3.0 mm, h_1 = 6.0 mm, h_2 = 15.0 mm, h_3 = 10.0 mm, W_1 = 13.0 mm, W_2 = 2.0 mm, and L_2 = 2.5 mm).

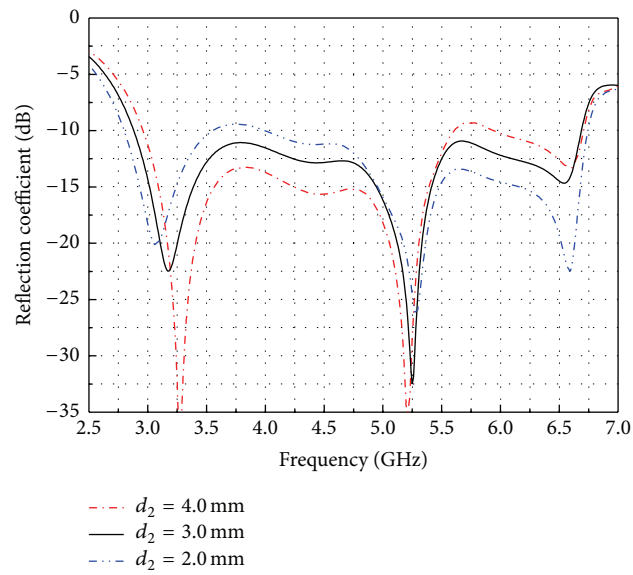

FIGURE 7: Simulated reflection coefficient with different values of d_2 (d_1 = 23.0 mm, h_1 = 6.0 mm, h_2 = 15.0 mm, h_3 = 10.0 mm, W_1 = 13.0 mm, W_2 = 2.0 mm, L_1 = 4.5 mm, and L_2 = 2.5 mm).

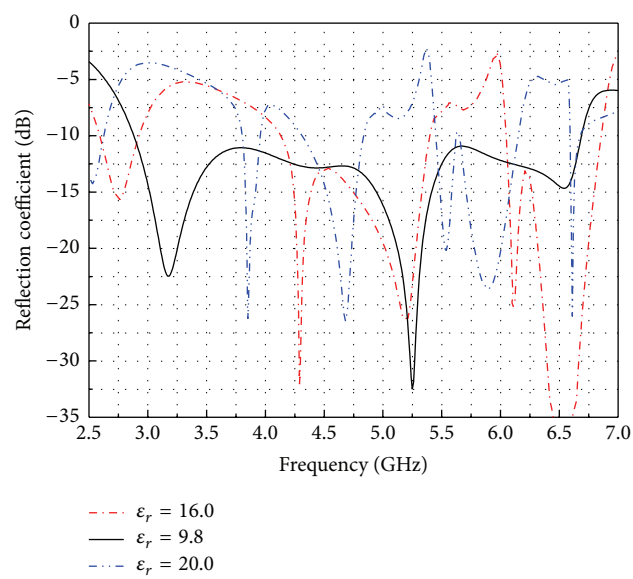

FIGURE 8: Simulated reflection coefficient with different values of ε_r (d_1 = 23.0 mm, d_2 = 3.0 mm, h_1 = 6.0 mm, h_2 = 15.0 mm, h_3 = 10.0 mm, W_1 = 13.0 mm, W_2 = 2.0 mm, L_1 = 4.5 mm, and L_2 = 2.5 mm).

Thus, the broad impedance bandwidth is achieved by coupling the resonant mode of the monopole patch and the fundamental mode of DR. The coupling between the DR and the feeding mechanism can be easily adjusted by changing the size of the feeding patch. Considering the overall performance, L_1 is chosen to be 4.5 mm, which has a better impedance matching than others.

3.3. The Notched Depth: d_2. Though the impedance matching is greatly improved by introducing an air gap and a modified trapezoidal feeding mechanism, the reflection coefficient is not good enough for wideband applications. In general, apart from h_1 and L_1, the notch dimension is another significant parameter. Therefore, in this part, the effect of the notched shape of the DRA is studied. The parametric study for various values of d_2 is shown in Figure 7. It is clear that when d_2 is 3.0 mm, the best impedance matching over the whole desired bandwidth has been achieved.

3.4. The DR Permittivity: ε_r. It is well known that as the dielectric constant is increased, the wavelength in the DR is decreased, rendering a lower resonant frequency. Figure 8

Figure 9: Photograph of the manufactured DRA.

shows the effect of the DR permittivity ε_r on the resonant frequencies. The increasing of the permittivity leads to the increasing of the Q-factor, hence reducing the bandwidth of the resonant modes. Note that the resonant frequency is greatly affected by the dielectric constant. As a result, a permittivity of $\varepsilon_r = 9.8$ is used to design the proposed DRA.

As mentioned above, the parameters of h_1, L_1, and d_2 are important and sensitive in tuning the dual resonant frequencies of the presented DRA. The dual resonant modes are as follows: one is from the feeding monopole patch and another is from the notched DR. Additionally, the DR permittivity has great influence on the achievable bandwidth.

4. Results and Discussion

To verify the proposed DRA design, an experimental prototype of the antenna has been fabricated and measured. The photograph of the manufactured DRA is shown in Figure 9. All the dimensions of the antenna are the same as in Table 1. The antenna performances in terms of the impedance bandwidth, the radiation patterns, antenna gain, and radiation efficiency were investigated experimentally.

The impedance bandwidth of the antenna was first examined, which was measured using an Agilent 8757D Network Analyzer. Figure 10 shows the measured and the simulated reflection coefficients (S_{11}) of the prototype DRA. It is seen that the simulated result agrees reasonably well with the measured one. If −10 dB reflection coefficient is chosen as reference, an impedance bandwidth of about 75% is achieved, which covers the frequency range from 2.9 GHz up to 6.7 GHz, where the antenna is resonant at the vicinity of 3.2 GHz and 5.3 GHz, respectively.

The radiation patterns were measured inside an anechoic chamber with the transmitting source antenna provided by a quad-ridge horn. The normalized radiation patterns of the proposed DRA, measured at several frequencies including 3.0 GHz, 5.0 GHz, and 6.5 GHz, are depicted in Figure 11. From an overall view of these radiation patterns, it can be seen that stable broadside patterns in both principle planes are obtained across the operating frequency band, which verifies the TE_{111} mode being excited. The desired TE_{111} mode is the fundamental mode of the DRA excited by the offset

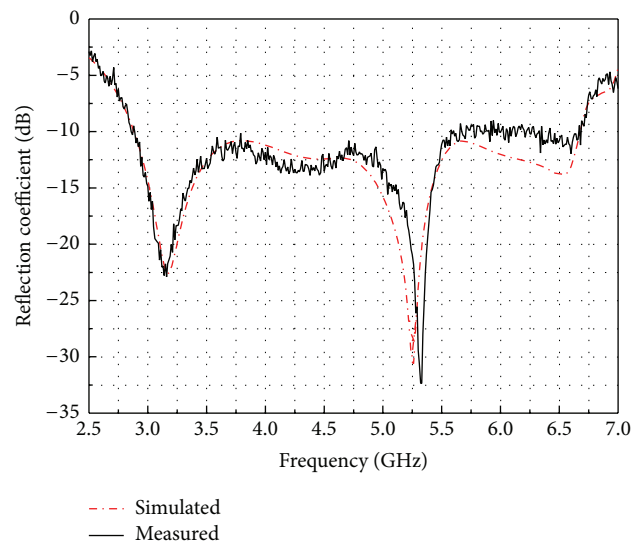

Figure 10: Measured and simulated reflection coefficient of the proposed DRA.

monopole patch. In reference to these curves, in the H-plane (xz-plane), the measured radiation patterns are symmetrical. However, in the E-plane (yz-plane), the radiation patterns are not symmetrical and have slight deformation at the higher band, which is mainly due to the effects of the higher order modes.

Figure 12 plots the measured and simulated peak gain of the proposed DRA. It is found that the gain range is about 4.8 dBi~6.5 dBi. Thus, the peak gain is stable within the operating frequency band. In addition, Figure 13 depicts the plot of the measured and simulated radiation efficiency versus the desired frequency. It can be noted from the results that the radiation efficiency is nearly more than 80%, so the DRA works with very high efficiency in the operation bandwidth. The highest radiation efficiency (~90%) is obtained at 5.0 GHz (i.e., second resonant point) due to good matching conditions. This is expected because DRAs have more radiation efficiency than conventional microstrip patch antennas [2].

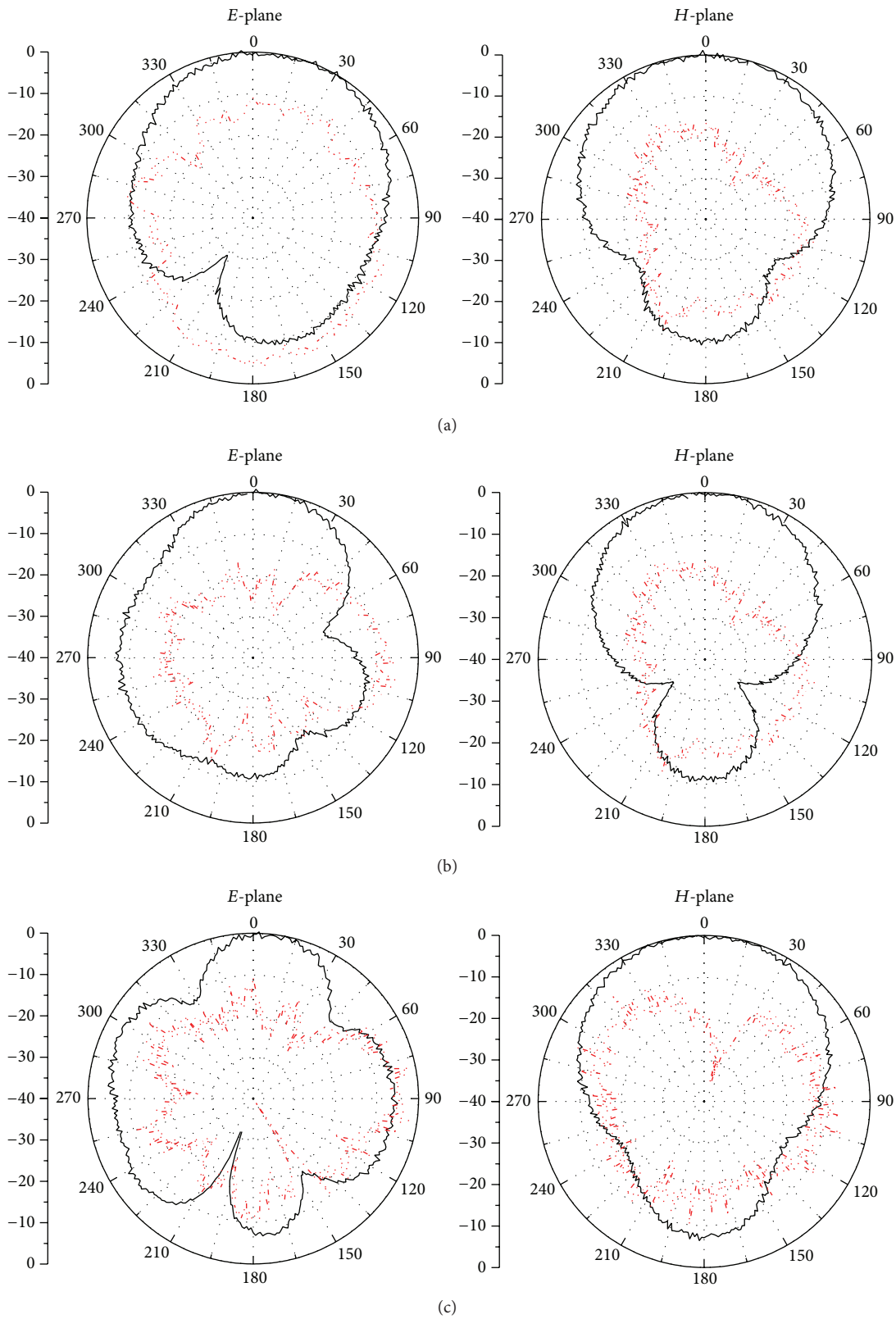

Figure 11: Measured normalized radiation patterns of the proposed DRA. (a) 3.0 GHz, (b) 5.0 GHz, and (c) 6.5 GHz.

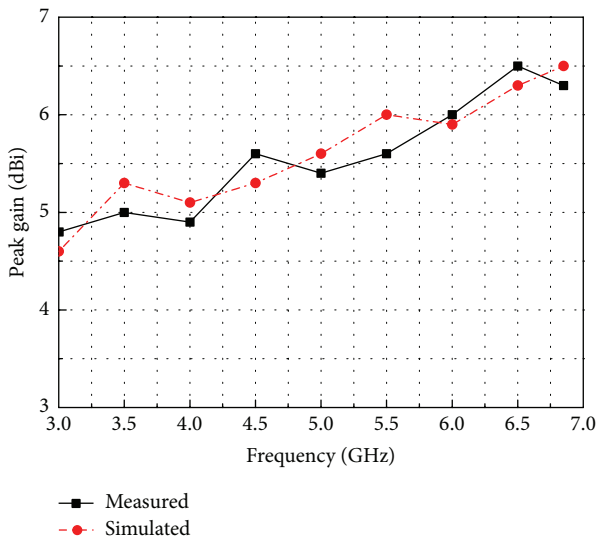

Figure 12: Measured and simulated peak gain of the proposed DRA.

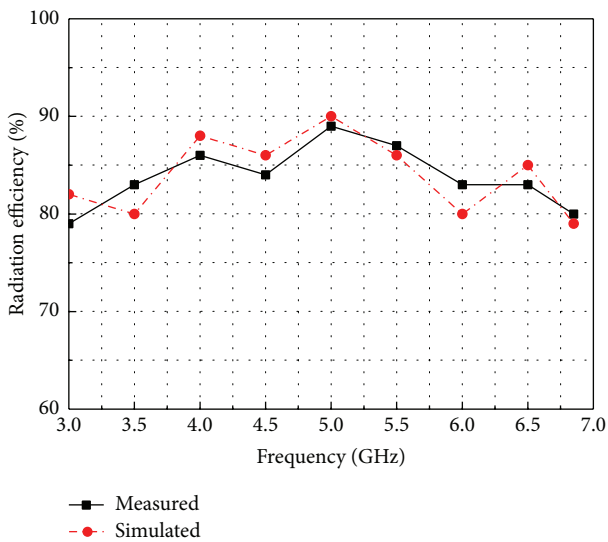

Figure 13: Measured and simulated radiation efficiency of the proposed DRA.

5. Conclusions

In this paper, a compact DRA with a trapezoidal monopole patch adhered on the DR concave surface as a feeding mechanism has been described and investigated for wideband applications. A parametric study is carried out to optimize the antenna design. From the simulated results obtained, it is observed that an air gap, the patch feed mechanism, and the shape of the DR are very important for improving the DRA bandwidth. The simulated and measured performances agree well, confirming the theoretical design. According to the measured results, it can be observed that the proposed DRA provides wide impedance bandwidth, consistent broadside radiation patterns, stable gain, and high radiation efficiency with compact size. Moreover, this DRA is simple in structure and easy to be fabricated. It is very attractive and can be practical in use for various wireless communication systems such as WiMAX (3.4 GHz~3.7 GHz) and WLAN (5.15 GHz~5.35 GHz). As a result, this antenna is a strong participant in the race of compact, wideband, and inexpensive antennas.

Competing Interests

The authors declare that there are no competing interests regarding the publication of this paper.

Acknowledgments

This work was funded by the National Natural Science Foundation of China (nos. 61101069 and 61201135), and it was supported in part by the Shaanxi Natural Science Foundation (no. 2015JQ6243).

References

[1] S. A. Long, M. W. McAllister, and L. C. Shen, "The resonant cylindrical dielectric cavity antenna," *IEEE Transactions on Antennas and Propagation*, vol. 31, no. 3, pp. 406–412, 1983.

[2] Q. Lai, G. Almpanis, C. Fumeaux, H. Benedickter, and R. Vahldieck, "Comparison of the radiation efficiency for the dielectric resonator antenna and the microstrip antenna at Ka band," *IEEE Transactions on Antennas and Propagation*, vol. 56, no. 11, pp. 3589–3592, 2008.

[3] X. S. Fang and K. W. Leung, "Designs of single-, dual-, wideband rectangular dielectric resonator antennas," *IEEE Transactions on Antennas and Propagation*, vol. 59, no. 6, pp. 2409–2414, 2011.

[4] A. Petosa and A. Ittipiboon, "Dielectric resonator antennas: a historical review and the current state of the art," *IEEE Antennas and Propagation Magazine*, vol. 52, no. 5, pp. 91–116, 2010.

[5] W. M. Abdel-Wahab, D. Busuioc, and S. Safavi-Naeini, "Millimeter-wave high radiation efficiency planar waveguide series-fed dielectric resonator antenna (DRA) array: analysis, design, and measurements," *IEEE Transactions on Antennas and Propagation*, vol. 59, no. 8, pp. 2834–2843, 2011.

[6] G. P. Junker, A. A. Kishk, A. W. Glisson, and D. Kajfez, "Effect of air gap on cylindrical dielectric resonator antenna operating in TM_{01} mode," *Electronics Letters*, vol. 30, no. 2, pp. 97–98, 1994.

[7] X.-L. Liang and T. A. Denidni, "H-shaped dielectric resonator antenna for wideband applications," *IEEE Antennas and Wireless Propagation Letters*, vol. 7, pp. 163–166, 2008.

[8] Q. Rao, T. A. Denidni, and A. R. Sebak, "Broadband compact stacked T-shaped DRA with equilateral-triangle cross sections," *IEEE Microwave and Wireless Components Letters*, vol. 16, no. 1, pp. 7–9, 2006.

[9] Y. Ge, K. P. Esselle, and T. S. Bird, "Compact dielectric resonator antennas with ultrawide 60%–110% bandwidth," *IEEE Transactions on Antennas and Propagation*, vol. 59, no. 9, pp. 3445–3448, 2011.

[10] T. A. Denidni, Z. Weng, and M. Niroo-Jazi, "Z-shaped dielectric resonator antenna for ultrawideband applications," *IEEE Transactions on Antennas and Propagation*, vol. 58, no. 12, pp. 4059–4062, 2010.

[11] Y. Coulibaly, T. A. Denidni, and H. Boutayeb, "Broadband microstrip-fed dielectric resonator antenna for X-band applications," *IEEE Antennas and Wireless Propagation Letters*, vol. 7, pp. 341–345, 2008.

[12] X.-L. Liang, T. A. Denidni, and L.-N. Zhang, "Wideband L-shaped dielectric resonator antenna with a conformal inverted-trapezoidal patch feed," *IEEE Transactions on Antennas and Propagation*, vol. 57, no. 1, pp. 271–273, 2009.

[13] L.-N. Zhang, S.-S. Zhong, and S.-Q. Xu, "Broadband U-shaped dielectric resonator antenna with elliptical patch feed," *Electronics Letters*, vol. 44, no. 16, 2008.

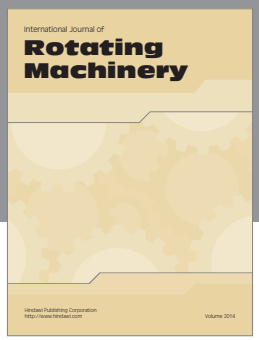

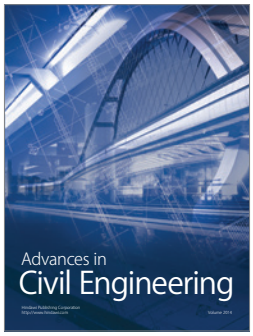

Hindawi

Submit your manuscripts at
http://www.hindawi.com